Journal of Zhejiang University-SCIENCE B (Biomedicine & Biotechnology)
ISSN 1673-1581 (Print); ISSN 1862-1783 (Online)
www.zju.edu.cn/jzus; www.springerlink.com
E-mail: jzus@zju.edu.cn

Spatial and seasonal characterization of net primary productivity and climate variables in southeastern China using MODIS data*

Dai-liang PENG[†1,2], Jing-feng HUANG[1,3,4], Alfredo R. HUETE[5], Tai-ming YANG[6], Ping GAO[7], Yan-chun CHEN[8], Hui CHEN[9], Jun LI[10], Zhan-yu LIU[†‡1,3,4]

(*[1]Institute of Agricultural Remote Sensing and Information Application, Zhejiang University, Hangzhou 310029, China*)
(*[2]Center for Earth Observation and Digital Earth, Chinese Academy of Sciences, Beijing 100190, China*)
(*[3]Ministry of Education Key Laboratory of Environmental Remediation and Ecological Health, Zhejiang University, Hangzhou 310029, China*)
(*[4]Key Laboratory of Agricultural Remote Sensing and Information System of Zhejiang Province, Hangzhou 310029, China*)
(*[5]Department of Soil, Water, and Environmental Science, University of Arizona, Tucson, AZ 85721, USA*)
(*[6]Institute of Anhui Meteorology, Hefei 230031, China*)
(*[7]Institute of Jiangsu Meteorology, Nanjing 210008, China*)
(*[8]Institute of Shandong Meteorology, Jinan 250031, China*)
(*[9]Institute of Fujian Meteorology, Fuzhou 350001, China*)
(*[10]Shanghai Climate Centre, Shanghai 200030, China*)
[†]E-mail: pdlzju@yahoo.com.cn; liuzhanyu@zju.edu.cn

Received Apr. 5, 2009; Revision accepted Oct. 23, 2009; Crosschecked Feb. 25, 2010

Abstract: We developed a sophisticated method to depict the spatial and seasonal characterization of net primary productivity (NPP) and climate variables. The role of climate variability in the seasonal variation of NPP exerts delayed and continuous effects. This study expands on this by mapping the seasonal characterization of NPP and climate variables from space using geographic information system (GIS) technology at the pixel level. Our approach was developed in southeastern China using moderate-resolution imaging spectroradiometer (MODIS) data. The results showed that air temperature, precipitation and sunshine percentage contributed significantly to seasonal variation of NPP. In the northern portion of the study area, a significant positive 32-d lagged correlation was observed between seasonal variation of NPP and climate (P<0.01), and the influences of changing climate on NPP lasted for 48 d or 64 d. In central southeastern China, NPP showed 16-d, 48-d, and 96-d lagged correlation with air temperature, precipitation, and sunshine percentage, respectively (P<0.01); the influences of air temperature and precipitation on NPP lasted for 48 d or 64 d, while sunshine influence on NPP only persisted for 16 d. Due to complex topography and vegetation distribution in the southern part of the study region, the spatial patterns of vegetation-climate relationship became complicated and diversiform, especially for precipitation influences on NPP. In the northern part of the study area, all vegetation NPP had an almost similar response to seasonal variation of air temperature except for broad crops. The impacts of seasonal variation of precipitation and sunshine on broad and cereal crop NPP were slightly different from other vegetation NPP.

Key words: Net primary productivity, Climate variables, Spatial characterization, Lagged cross-correlation, Moderate-resolution imaging spectroradiometer, Geographic information system technology
doi:10.1631/jzus.B0910501 **Document code:** A **CLC number:** TP7; P4

1 Introduction

Terrestrial net primary production (NPP) plays a very important role in essential materials and suitable environments for human society (Peng and Apps, 1999; Zhao *et al*., 2005). Recently, NPP has been studied as a significant component in the ecosystem processes, which stores carbon dioxide (CO_2) in the living tissue from atmosphere (Canadell *et al*., 2000; Ahl *et al*., 2004), and a clear and concise description for the correlation between NPP and climate change is crucial for the research on the relationship between

‡ Corresponding author
* Project supported by the National High-Tech Research and Development Program (863) of China (No. 2006AA120101), the National Natural Science Foundation of China (Nos. 40871158 and 40875070), and the Key Technologies Research and Development Program of China (No. 2006BAD10A01)

global climate change and carbon cycling processes (Steele *et al*., 2005; Zhang *et al*., 2002).

NPP is controlled by many natural and anthropogenic factors, and climate plays a major role in NPP spatial and temporal variation (Field *et al*., 1995). Climate impact on NPP is not only related to climatic variables, but also to different temporal dimensions (Steele *et al*., 2005; Peng *et al*., 2008). NPP inter-annual fluctuations of different magnitudes exist because of global climate anomalies (Maisongrande *et al*., 1995; Kindermann *et al*., 1996; Malmström *et al*., 1997; Mohamed *et al*., 2004). In short time scales, climate variables such as air temperature, precipitation and sunshine hours directly affect the physiological processes, including stomatal conductance, plant photosynthesis and respiration (Field *et al*., 1995). Consequently, the study of the seasonal patterns of NPP and its relationship to climate variables is very important for strengthening the understanding of NPP-climate relationships. The impact of seasonal changes of climate on NPP was delayed and persisted for some time (Peng *et al*., 2008), yet the relative importance of climate factors and NPP is that they are the geographical variables (Running *et al*., 2004). Hence, it is necessary to study the spatial characterization of the relationship between seasonal variation of NPP and climate. The integration of remote sensing data and geographic information system (GIS) technology provides a potential approach to this study (Abdallah *et al*., 2005; López-Blanco and Villers-Ruiz, 1995; Wang *et al*., 2008).

The purpose of this work is to extend and adapt the lagged cross-correlation analysis method, to study the delayed and continuous effects of seasonal climate on NPP, and to map the spatial and seasonal characterization of NPP and climate variables using GIS technology. We developed our approach in southeastern China using moderate-resolution imaging spectroradiometer (MODIS) data.

2 Materials and methods

2.1 Study area

Southeastern China, located between 23°–38° N and 114°–123° E (Fig. 1), was selected to study the spatial characterization of NPP and climate relationships. This region belongs to the monsoon climate area of a warm temperate zone. The total land area is about 605 800 km^2, of which 54.55% is crop land (including 41.95% cereal crops and 12.60% broad crops), 15.14% evergreen forests, 14.79% deciduous forests, 5.28% grass, 4.58% shrub, 2.16% water, and 3.23 % urban (Fig. 1).

2.2 Data

MODIS 16-d composite data at 250 m spatial resolution (MOD13Q1) from 2001 to 2004 were collected from the Earth Observing System Data Gateway. Each composite MOD13Q1 pixel is temporally filtered to the closest nadir view angle, with the least cloud or cloud shadow, and the lowest aerosol loading (Huete *et al*., 2002; Sun *et al*., 2009). MODIS land cover product (500 m spatial resolution), which incorporates five different land cover classification schemes, was used to analyze the land cover distribution within the study area. Some vegetation types within the International Geosphere Biosphere Programme (IGBP) classification occupy a small region in southeastern China. Consequently, the fifth land cover scheme classification was used and subsequently reclassified as six vegetation types (cereal crops, broad crops, evergreen forests, deciduous forests, grass and shrub). Moreover, the area of each vegetation type had a very slight difference between 2001 and 2004. To study the impact of climate change on seasonal variation in NPP accurately, the highest quality MODIS data over a four-year period were selected using quality assurance information.

Daily average air temperature, total precipitation, average vapor pressure, sunshine percentage and average wind speed data from 2001 to 2004 were collected from 307 meteorological stations. For each climate variable, the values were calculated with the same temporal resolution as MODIS normalized difference vegetation index (NDVI). Longitude, latitude, elevation and the distance from the coast were selected as major factors relating to the spatial distribution of climate variables. Grid maps of each climate factor were obtained by trend surface analysis and residual interpolation method (Yu *et al*., 2004; Liu *et al*., 2004; Li, 2006; Peng *et al*., 2007b). Meteorological data from 227 stations were used for modeling, and data from the remaining stations were used for validation. Relative errors for each climate variable were less than 5% over 96% of southeastern China regions and less than 10% in the remaining study areas. The absolute errors of air temperature, precipitation, sunshine percentage, vapor pressure and wind speed were 0.5 °C, 2.0 mm, 0.013, 0.4 hPa and 0.0006 m/s, respectively.

2.3 NPP estimation

There are three types of models generally used to calculate NPP, including statistical model, parametric model, and ecological process model (Ruimy *et al*., 1999), and the integration of parametric and process models, which is an effective method to combine remote sensing data with ecological/biophysical processes, has been used to estimate global and regional NPP (Bartelink *et al*., 1997; Peng *et al*., 2008). The algorithms are defined as follows:

$$\mathrm{NPP}=\mathrm{GPP}-(R_\mathrm{m}+R_\mathrm{g}), \quad (1)$$

where GPP is gross primary productivity [g C/(m^2·16 d)], and R_m and R_g are the maintenance and growth respiration by all living parts including fine roots and leaves [g C/(m^2·16 d)], respectively.

$$\mathrm{GPP}=\varepsilon_\mathrm{g}\times\mathrm{FPAR}\times\mathrm{PAR}\times f_1(T)\times f_2(\beta), \quad (2)$$

where ε_g is the light use efficiency, ε_g=2.76 g C/MJ in this study; PAR is the photosynthetically active radiation [MJ/(m^2·16 d)]; FPAR is the fraction of absorbed PAR and can be calculated by vegetation index (VI) and the maximum and minimum FPARs; $f_1(T)$ and $f_2(\beta)$ account for stresses induced by temperature and soil water availability, respectively (Field *et al*., 1995; Sun, 1998; Sun and Zhu, 2001; Turner *et al*., 2002; Zhao *et al*., 2005).

$$\mathrm{FPAR}=\frac{(\mathrm{VI}-\mathrm{VI}_{i,\min})\times(\mathrm{FPAR}_{\max}-\mathrm{FPAR}_{\min})}{\mathrm{VI}_{i,\max}-\mathrm{VI}_{i,\min}}+\mathrm{FPAR}_{\min} \quad (i=1,2,\ldots,23), \quad (3)$$

$$\mathrm{VI}=(1+\mathrm{NDVI})/(1-\mathrm{NDVI}), \quad (4)$$

where $\mathrm{FPAR}_{\max}$=0.950 and $\mathrm{FPAR}_{\min}$=0.001. $\mathrm{NDVI}_{i,\max}$ and $\mathrm{NDVI}_{j,\min}$ for different vegetation types are shown in Table 1 (Sun, 1998).

$$\mathrm{PAR}=0.47(C_{0i}+C_{1i}\mathrm{lat}+C_{2i}H+C_{3i}e_\mathrm{d})\times(0.207+0.725S), \quad (5)$$

where lat is latitude (°), H is altitude (m), e_d and S are the 16-d average vapor pressure (hPa) and sunshine percentage, and C_{0i}, C_{1i}, C_{2i} and C_{3i} are the model parameter coefficients as shown in Table 2 (Hou *et al*., 1993).

Table 1 $\mathrm{NDVI}_{i,\max}$ and $\mathrm{NDVI}_{j,\min}$ for different vegetation types

Vegetation type	$\mathrm{NDVI}_{i,\max}$	$\mathrm{NDVI}_{j,\min}$
Evergreen forests	0.721	0.039
Deciduous forests	0.689	0.039
Grass	0.611	0.039
Shrub	0.674	0.039
Crops	0.674	0.039

Table 2 C_{0i}, C_{1i}, C_{2i} and C_{3i} values

i	C_{0i}	C_{1i}	C_{2i}	C_{3i}
1	23 120.600	−354.568	0.427	−128.731
2	23 120.600	−354.568	0.427	−128.731
3	22 379.700	−279.973	0.405	−158.028
4	22 379.700	−279.973	0.405	−158.028
5	25 758.200	−222.744	0.513	−170.840
6	25 758.200	−222.744	0.513	−170.840
7	26 004.200	−137.346	0.469	−144.467
8	26 004.200	−137.346	0.469	−144.467
9	26 802.200	−63.730	0.472	−119.828
10	26 802.200	−63.730	0.472	−119.828
11	22 802.100	25.106	0.705	−45.246
12	22 802.100	25.106	0.705	−45.246
13	22 379.100	26.478	0.876	−11.659
14	22 379.100	26.478	0.876	−11.659
15	21 569.300	−31.205	1.037	−22.191
16	21 569.300	−31.205	1.037	−22.191
17	23 208.500	−153.511	0.710	−28.131
18	23 208.500	−153.511	0.710	−28.131
19	28 193.400	−336.725	0.250	−163.196
20	28 193.400	−336.725	0.250	−163.196
21	23 275.500	−338.163	0.370	−92.329
22	23 275.500	−338.163	0.370	−92.329
23	22 878.700	−368.903	0.380	−109.287

$$f_1(T)=1/[(1+\mathrm{e}^{4.5-T})(1+\mathrm{e}^{T-37.5})], \quad (6)$$

$$f_2(\beta)=0.5+0.5\beta, \quad (7)$$

$$\beta=\min(W_i/(0.75W_\mathrm{Fc}), 1), \quad (8)$$

$$W_i=\min\left(W_{i-1}+\mathrm{PT}_i-\min\left(\frac{W_i}{0.75W_\mathrm{FC}},1\right)\times\mathrm{ET_P},W_\mathrm{FC}\right), \quad (9)$$

where T and $\mathrm{ET_p}$ are the 16-d average air temperature (°C) and potential evapotranspiration (hPa), respectively; PT_i is the precipitation (mm) summed over a 16-d period and W_i is the soil water content (mm), i=1, 2, …, 23; W_FC is the field water capacity (Table 3) (Sun, 1998).

Table 3 Field water capacity for different soil texture

Soil texture	Field water capacity
Coarse sand soil	0.170
Fine sand soil	0.230
Facet sand soil	0.260
Sandy silt soil	0.360
Silt soil	0.410
Sandy loam soil	0.320
Loam soil	0.400
Sandy clay soil	0.300
Silt clay soil	0.400
Loam clay soil	0.420
Clay soil	0.480

$$\mathrm{ET_p}=\frac{\Delta Q_\mathrm{n}+\gamma E_\mathrm{a}}{\Delta+\gamma}, \tag{10}$$

where Δ is the saturated vapor pressure curve slope, Q_n, E_a, and γ are the radiation balance [J/(m^2·16 d)], air dryness, and psychrometric constant, respectively.

$$\begin{aligned}Q_\mathrm{n}=&1.7\mathrm{PAR}-5.6696\times10^{-8}(273+T)^4\times\\&(0.56-0.08\sqrt{e_\mathrm{d}})\times(0.1+0.9S),\end{aligned} \tag{11}$$

$$E_\mathrm{a}=0.26(1+0.0757U)\times(6.11\times10^{7.5T/(237.3+T)}-e_\mathrm{d}), \tag{12}$$

$$\gamma=0.668\times10^{-H/[18400(1+T/273)]}, \tag{13}$$

where PAR can be calculated from Eq. (5), and U is wind speed (m/s).

$$R_\mathrm{m}=(1+\mathrm{NDVI}/\mathrm{NDVI}_\mathrm{max})\times MR_\mathrm{m0}2.0^{(T-20)/10}, \tag{14}$$

$$R_\mathrm{g}=0.25(\mathrm{GPP}-R_\mathrm{m}), \tag{15}$$

where M and R_{m0} are the dry matter weight (g C/m^2) and coefficient of maintenance respiration as shown in Table 4 (Lieth, 1975; Foley, 1994; Hunt, 1994; Bonan, 1995).

Table 4 Dry matter weight (*M*) and the fraction of maintenance respiration (R_{m0}) for different vegetation types

Vegetation type	M (g C/m^2)	R_{m0} ((16 d)$^{-1}$)
Evergreen forests	20000	0.003328
Deciduous forests	17000	0.003328
Grass	500	0.003328
Shrub	4000	0.012672
Crops	600	0.033328

2.4 Regression and lagged cross-correlation analysis

We extracted NPP and three climate variables within areas of six vegetation types (cereal crops, broad crops, evergreen forests, deciduous forests, grass, and shrub). The correlation between NPP and air temperature, precipitation and sunshine percentage for each vegetation type was analyzed.

We adopted an assumption that if the correlation between the coefficient of variations (CV) of NPP and climate factors was significant, the seasonal fluctuation of NPP is attributed to these climate variability (Fang *et al*., 2001).

Lagged cross-correlation analysis incorporates both immediate physiological alterations and delayed biogeochemical adjustments of vegetation because of variable climates (Mohamed *et al*., 2004; Steele *et al*., 2005; Peng *et al*., 2007a). The response of NPP to climate change is not instantaneous and has important delayed and continuous effects. The method of time-lagged correlation analysis is defined as follows (Fik and Mulligan, 1998; Zhang *et al*., 2005; Peng *et al*., 2008):

$$r_k(x,y)=S_k(x,y)/S_xS_{y+k}, \tag{16}$$

where $S_k(x, y)$ is the sample covariance; S_x, S_{y+k} are the standard deviations and they are calculated by the following equations:

$$\begin{cases}S_k(x,y)=\dfrac{1}{n-k}\sum\limits_{i=1}^{n-k}(x_i-\overline{x}_i)(y_{i+k}-\overline{y}_{i+k}),\\ S_x=\left[\dfrac{1}{n-k}\sum\limits_{i=1}^{n-k}(x_i-\overline{x}_i)^2\right]^{1/2},\\ S_{y+k}=\left[\dfrac{1}{n-k}\sum\limits_{i=1}^{n-k}(y_{i+k}-\overline{y}_{i+k})^2\right]^{1/2}.\end{cases} \tag{17}$$

$\overline{x}_i$, $\overline{y}_i$ are defined as follows:

$$\begin{cases}\overline{x}_i=\dfrac{1}{n-k}\sum\limits_{i=1}^{n-k}x_i,\\ \overline{y}_i=\dfrac{1}{n-k}\sum\limits_{i=1}^{n-k}y_{i+k},\end{cases} \tag{18}$$

where n is the degree of freedom (df) for x_i and y_i, $k \le n/4$; in this study, n equals 23, so k is 0, 1, 2, 3, 4, and 5. The critical values of the significant positive correlation coefficients ($P<0.01$) are 0.51, 0.52, 0.53, 0.54, 0.55 and 0.56 when k equals 0, 1, 2, 3, 4 and 5, respectively. If the value of the correlation coefficient (R_k) is greater than the corresponding critical value, and R_k is the maximal correlation coefficient at different time lags, then the time lag equals k times 16 d.

The impact of climate change on NPP may persist for a long time. In this paper, the duration of climate influence on NPP was calculated by the following method. If R_k and R_{k+1} are greater than the corresponding critical values of significant correlation coefficients ($P<0.01$), the duration length of climate influence is 16 d. If R_k, R_{k+1} and R_{k+2} are greater than the critical values of significant correlation coefficients ($P<0.01$), indicating that the duration length of climate influence is 32 d, other duration lengths can be achieved by analogy with this method.

3 Results

3.1 NPP validation and their seasonal patterns

NPP from previous work and measured values were used to assess the accuracy of estimating NPP using the above algorithms (Table 5). NPP values for evergreen and deciduous forests are similar to the results of other studies and measured values. Crops and shrub NPP values lie within the ranges of the Sun and Zhu (2000)'s study, and grass NPP values are close to MODIS NPP and measured values. In addition, the annual NPP values show a significant positive spatial correlation with MODIS NPP ($P<0.01$).

The seasonal patterns of NPP for each vegetation type are shown in Fig. 2. The minimum and maximum values of NPP appear in winter and summer, respectively. However, the maximum NPP values of winter wheat appear in spring because of paddy-rice and upland crop (e.g., winter wheat, rapeseed) rotation. Evergreen forests have the highest NPP value, followed by deciduous forests. Moreover, the NPP values of grass and shrub are lower than those of other vegetation because of the sparse distribution of grass and shrub within the study area.

3.2 Correlation between seasonal variation of NPP and climate variables

The CVs of NPP exhibited significant positive correlations with the CVs of air temperature and precipitation ($P<0.01$), and a significant negative correlation with the CV of sunshine percentage ($P<0.01$) (Table 6). These data indicate that the seasonal fluctuation in NPP is attributed to air temperature, precipitation and sunshine percentage in southeastern China. Therefore, the relative variation in air temperature and precipitation determines the seasonal fluctuation of NPP, and sunshine percentage variability is inversely correlated to the variability of NPP. The negative and positive correlations with air temperature, precipitation and sunshine percentage reflect the impacts from increase and decrease of water loss on vegetation production (Mohamed *et al*., 2004).

3.3 Spatial characterization of delayed and continuous effects of seasonal climate variability on NPP

3.3.1 Air temperature

Based on the results of lagged cross-correlation analysis, we calculated the area percentages of air temperature influences on NPP at different time lags and duration lengths (Tables 7–8). The spatial distribution of the time lags and duration lengths of air temperature influences on NPP is shown in Fig. 3. NPP for other vegetation types had a similar response to seasonal variation of air temperature, except for broad crops in the northern portion of the study area.
There were only 1% of areas where NPP had no correlation with seasonal air temperature change. A significant positive 16-d lagged correlation between seasonal air temperature and NPP was observed in most portions of southern and middle southeastern China. 22% cereal crop, 30% broad crop, 11% evergreen and deciduous forests, and 16% shrub and grass NPP showed a significant positive 32-d lagged correlation with air temperature ($P<0.01$). Most of the vegetation was distributed in Shandong and Jiangsu Provinces. In the northern Shandong Province, crop NPP had a significant positive 48-d lagged correlation with air temperature ($P<0.01$) (Table 7, Fig. 3a).

Table 5 Inter-comparison among several estimating NPP results

Vegetation type	NPP [g C/(m^2·a)]				
	This study	MODIS NPP	Sun and Zhu (2000)	Mohamed *et al.* (2004)	Measured values (Liu *et al.*, 1993; Hu *et al.*, 1990)
Evergreen forests	1000.03	951.04	529.40–971.90	1019.00	160.00–1340.00
Deciduous forests	791.96	751.31	419.86–459.70	711.00	150.00–700.00
Shrub	497.44	516.49	290.17–555.42		
Grass	259.18	248.30	116.03–191.41	352.00	66.00–240.00
Crops	356.33	241.11	313.31–396.36	426.00	

Table 6 Correlation coefficients between the CVs of NPP and those of climate variables

Climatic factor	Cereal crops	Broad crops	Evergreen forests	Deciduous forests	Shrub	Grass
Air temperature	0.79*	0.87*	0.75*	0.75*	0.73*	0.74*
Precipitation	0.63*	0.76*	0.57*	0.55*	0.54*	0.54*
Sunshine percentage	−0.66*	−0.76*	−0.65*	−0.64*	−0.57*	−0.61*

* Significance of the trends at $P<0.01$

Table 7 Area percentage of air temperature influences on NPP at different time lags in southeastern China

Vegetation type	Area percentage (%)						
	0 d	16 d	32 d	48 d	64 d	80 d	96 d
Cereal crops	0.00	74.64	21.77	3.00	0.13	0.08	0.39
Broad crops	0.00	64.78	29.53	5.15	0.19	0.10	0.25
Evergreen forests	0.00	87.77	10.69	1.08	0.08	0.13	0.25
Deciduous forests	0.00	88.18	10.46	0.93	0.07	0.13	0.24
Shrub	0.00	82.10	15.37	1.82	0.20	0.12	0.40
Grass	0.00	81.03	16.35	1.90	0.20	0.13	0.39

Table 8 Area percentage of air temperature influences on NPP with different duration lengths in southeastern China

Vegetation type	Area percentage (%)						
	Non-correlation	16 d	32 d	48 d	64 d	80 d	96 d
Cereal crops	1.30	0.64	4.76	32.63	56.34	3.68	0.65
Broad crops	0.85	0.70	5.56	23.33	62.02	6.54	1.00
Evergreen forests	1.34	0.54	3.66	44.04	49.16	1.16	0.11
Deciduous forests	1.30	0.44	3.55	43.93	49.54	1.16	0.09
Shrub	1.61	0.56	3.41	39.15	52.82	1.99	0.45
Grass	1.68	0.55	3.20	37.51	54.45	2.06	0.55

In the coastal areas of Jiangsu, Zhejiang and Fujian Provinces, the influences of seasonal air temperature on NPP persisted for 48 d. However, the duration length of air temperature influences on NPP was 64 d over most of the study area, which was mainly distributed in Shandong, Anhui and Fujian Provinces, and included 63% of cereal crops, 56% of broad crops, 50% of evergreen and deciduous forests, and 53% of shrub and grass. In addition, the influences of seasonal air temperature on NPP lasted for 80 d in the northern portion of Shandong Province (Table 8, Fig. 3b).

3.3.2 Precipitation

The statistical results of area percentages of precipitation influences on NPP at different time lags and duration lengths are shown in Tables 9 and 10. We mapped the spatial distribution of these results using GIS technology (Fig. 4). The significant influences of the seasonal precipitation change on crop NPP primarily occurred at 32-d or 48-d lag, and lasted for 48 d or 64 d. However, the NPP of all other vegetation types showed a significant correlation with precipitation at several different time lags. Moreover, the time lengths of precipitation influences had a dispersed distribution ranging from 16 d to 80 d.

In a few places in the western Anhui and Fujian Provinces, NPP had no correlation with precipitation. In the northern portion of the study area and the coastal areas of Zhejiang and Fujian Provinces, there was a significant positive 32-d lagged correlation between seasonal precipitation and NPP. Vegetation NPP showed a 48-d lagged correlation with precipitation in the middle portion of southeastern China, and a 64-d or 80-d lagged correlation in the western area of Fujian Province (Table 9, Fig. 4a).

The influences of precipitation persisted for 16 d or 32 d in some regions of the southern and central study area, and 48 d in Jiangsu and Shandong Provinces. In the northern portion of southeastern China, precipitation influences on NPP lasted for 64 d. However, some areas in the western Zhejiang and Fujian Provinces, precipitation influences on NPP lasted for up to 80 d (Table 10, Fig. 4b).

Precipitation infiltrates into the subsurface soil, and is absorbed by the roots of vegetation and subsequently stored by the vegetation canopy and stems, resulting in plants growth. These processes may contribute to the significant time lagged correlation and time lengths of precipitation influences on NPP.

3.3.3 Sunshine percentage

Sunshine percentage is calculated by the ratio of the actual measured sunshine hours to the maximum possible sunshine hours (Jensen *et al*., 1990). Sunshine influences on NPP differed from air temperature and precipitation. There was no significant correlation between seasonal NPP and sunshine percentage in the northwestern part of the study area, and a significant negative correlation was observed in other areas (Table 12, Fig. 5). These phenomena may be attributed to excess sunshine which results in water evaporation and vegetation water stress in southeastern China.

The significant correlation between seasonal sunshine percentage and crop NPP was observed at 16-d, 32-d, 48-d, and 96-d lags. NPP for all non-crop vegetation showed a significant correlation with seasonal sunshine percentage change at 16-d or 96-d lag (Table 11).

From south to north, the time lags of sunshine influences on NPP were 16, 80, 90, 32 and 48 d, respectively (Table 11, Fig. 5a). These influences lasted for 16 d over most southern and central areas of southeastern China, and 32 d in some areas in Zhejiang and Jiangsu Provinces. However, the effects of sunshine persisted for up to 48 d or 32 d in the northeastern portion of Shandong Province (Table 12, Fig. 5b).

Table 9 Area percentage of precipitation influences on NPP at different time lags in southeastern China

Vegetation type	Area percentage (%)						
	0 d	16 d	32 d	48 d	64 d	80 d	96 d
Cereal crops	0.00	3.33	53.92	31.09	5.66	4.95	1.06
Broad crops	0.00	4.84	67.77	17.20	4.26	5.26	0.66
Evergreen forests	0.00	1.67	33.75	33.47	15.60	13.73	1.77
Deciduous forests	0.00	1.81	33.98	33.22	15.57	13.61	1.82
Shrub	0.00	3.02	39.84	32.51	12.01	11.07	1.55
Grass	0.00	3.00	42.11	32.36	10.69	10.38	1.47

Table 10 Area percentage of precipitation influences on NPP with different duration lengths in southeastern China

Vegetation type	Area percentage (%)						
	Non-correlation	16 d	32 d	48 d	64 d	80 d	96 d
Cereal crops	3.21	6.52	13.88	33.18	38.21	4.67	0.34
Broad crops	2.69	7.73	11.40	32.80	42.12	3.11	0.15
Evergreen forests	7.51	14.00	20.98	19.93	27.48	9.77	0.31
Deciduous forests	8.03	14.18	20.89	19.89	26.87	9.80	0.34
Shrub	6.34	12.48	18.61	24.01	30.31	7.88	0.37
Grass	5.91	11.94	17.92	25.32	30.98	7.53	0.38

Table 11 Area percentage of sunshine influences on NPP at different time lags in southeastern China

Vegetation type	Area percentage (%)						
	0 d	16 d	32 d	48 d	64 d	80 d	96 d
Cereal crops	0.00	26.91	14.80	16.58	0.49	8.07	33.15
Broad crops	0.00	31.61	27.11	28.24	0.24	4.24	8.56
Evergreen forests	0.00	50.17	1.86	1.29	0.84	13.03	32.81
Deciduous forests	0.00	50.36	2.19	1.03	0.85	12.91	32.65
Shrub	0.00	44.76	6.44	5.79	0.73	11.39	30.89
Grass	0.00	43.10	7.77	6.93	0.59	10.85	30.75

Table 12 Area percentage of sunshine influences on NPP with different duration in southeastern China

Vegetation type	Area percentage (%)						
	Non-correlation	16 d	32 d	48 d	64 d	80 d	96 d
Cereal crops	43.10	36.78	11.54	8.00	0.56	0.01	0.00
Broad crops	41.69	28.86	13.59	14.93	0.92	0.02	0.00
Evergreen forests	31.95	59.11	7.79	1.09	0.06	0.00	0.00
Deciduous forests	31.36	59.50	7.77	1.31	0.07	0.00	0.00
Shrub	33.96	52.75	9.13	3.70	0.46	0.00	0.00
Grass	34.76	50.82	9.51	4.36	0.55	0.00	0.00

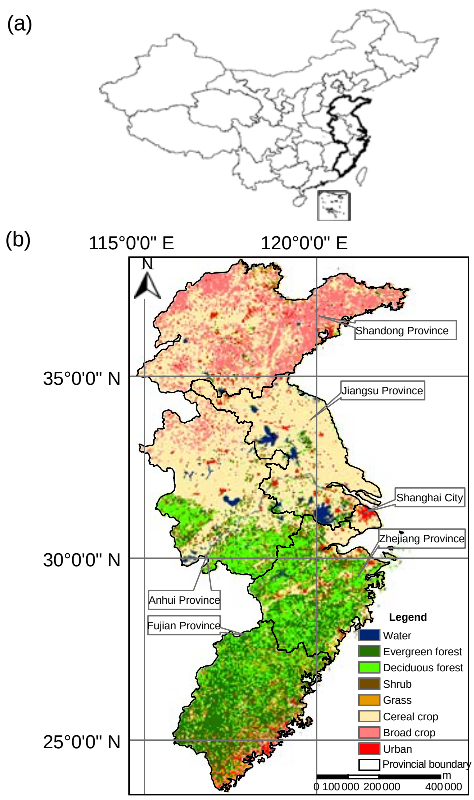

Fig. 1 The study area location in China (a) and land cover distribution (b)

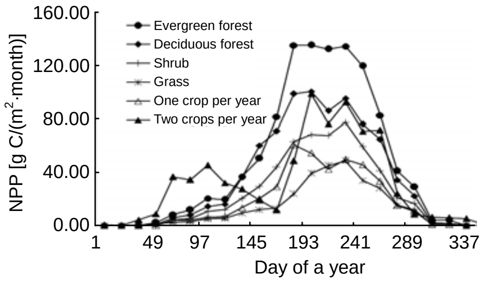

Fig. 2 Seasonal variation of NPP for different vegetation types

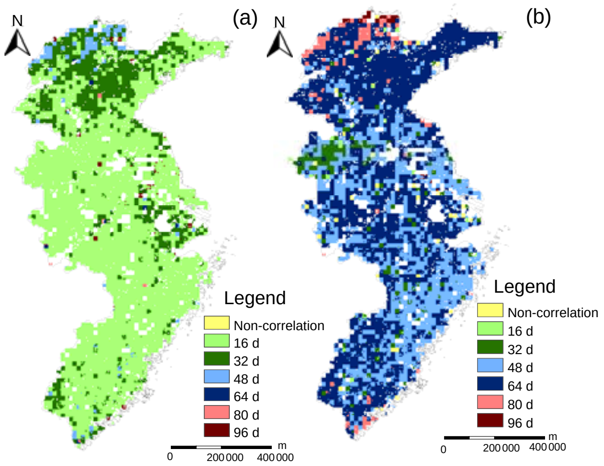

Fig. 3 Spatial distribution for time lags (a) and duration lengths (b) of air temperature influences on NPP

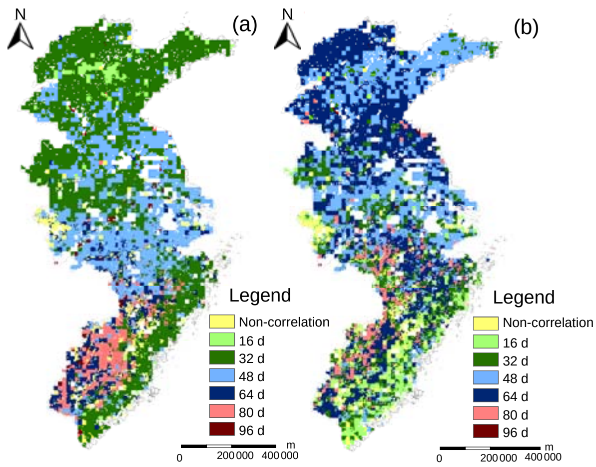

Fig. 4 Spatial distribution for time lags (a) and duration lengths (b) of precipitation influences on NPP

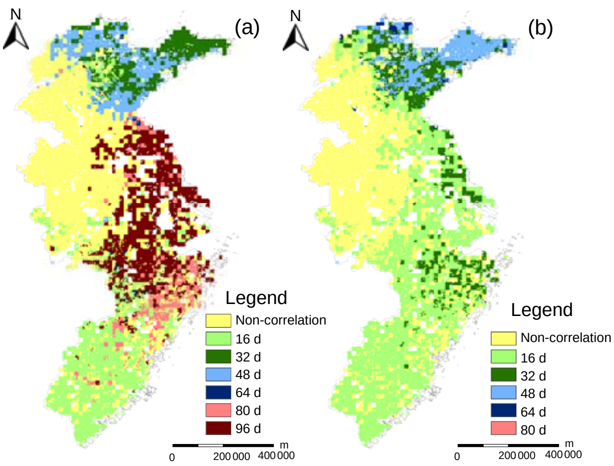

Fig. 5 Spatial distribution for time lags (a) and duration lengths (b) of sunshine percentage influences on NPP

4 Discussion

Southeastern China was selected as the study area because of its large latitude span, high vegetation coverage (about 95%), and spatial variation of vegetation types and climate. However, shrub and grass are dispersed throughout the study region, especially in the forests. They occupy about 10% of the study area. Therefore, it is very difficult to capture the different responses of shrub and grass NPP to the seasonal climate change from forests. The spatial and seasonal patterns of NPP and vegetation-climate relationship at a continental and global scale remain to be studied. Due to some uncertainties in the input data, the global seasonal MODIS NPP product is still being researched (Zhao *et al*., 2005; Zhao and Running, 2006). In addition, the temporal resolution of MODIS data in this study is 16 d, indicating that the error ranges of the time lags and duration lengths of the climate influences on NPP are 0 to 16 d. However, based on the lagged cross-correlation analysis method and GIS technology, with the update of MODIS products, acceptable spatial and temporal resolution MODIS data (such as MODIS combined products) and seasonal MODIS NPP will be favorable to the further vegetation-climate relationship studies at a continental or global scale.

NPP is driven by solar radiation and can be constrained by temperature, precipitation and sunshine (Lieth, 1975). This study used lagged cross-correlation analysis to explore the relationship between seasonal NPP and climate change. The spatial patterns of the vegetation-climate relationship were analyzed using GIS technology. Compared with previous researches, this study expands in the following three areas.

Firstly, Mohamed *et al*. (2004) studied the role of climate variability in the inter-annual variation of NPP. Annual NPP is the summation of seasonal NPP, and the response of annual NPP to climate change is also the cumulative effect of seasonal climate change. In addition, NPP is the main cause of seasonal fluctuations in atmospheric CO_2 concentrations (Ciais *et al*., 1995; Keeling *et al*., 1996). For estimates of the global carbon balance, a large amount of uncertainty centers on the role of terrestrial ecosystems. NPP and its corresponding seasonal variations are key components in the terrestrial carbon cycle. NPP seasonal fluctuations are vital to enhance our understanding of both the functioning of living ecosystems and subsequent feedback to the environment (Wolfgang, 1999).

Secondly, the continuous effect of climate variability on NPP was studied. The impact of climate on NPP is not instantaneous. However, it persists for a period of time (Fik and Mulligan, 1998). Under warm temperature, more vegetation growth causes more biomass input to the soil pool, and the associated precipitation causes high soil moisture, which facilitates the transformation of organic matter into readily available inorganic nutrients (mainly phosphorous and nitrogen) for the benefit of delayed plant growth (Neill *et al*., 1995; Tian *et al*., 1998). These processes may contribute to the delayed and continuous effects of climate on NPP.

Thirdly, the spatial patterns of the vegetation-climate relationship were mapped using GIS technology. As both NPP and climate have geographical variability (Running *et al*., 2004), the general descriptions are not sufficient to depict the vegetation-climate relationship, especially for a large study area.

5 Conclusion

This paper explored the spatial and seasonal characterization of NPP and climate variables. The significant correlations between the CVs of NPP and those of air temperature, precipitation and sunshine percentage indicated that the seasonal variation of NPP was attributed to the seasonal climate variability. We found that the responses of seasonal NPP to climate change were not only related to different climate factors, but also to the spatial distribution of these variables and different vegetation types. NPP had a significant positive correlation with air temperature and precipitation in almost all area of southeastern China. No significant correlation between vegetation NPP and seasonal sunshine fluctuations was observed in one third of the study area, and a significant negative correlation occurred in the remaining regions. In addition, the delayed and continuous effects of seasonal climate change on crop NPP were slightly different from other vegetation NPP.

6 Acknowledgement

We acknowledge the data support from the local meteorological departments in southeastern China, National Bureau of Statistics of China and Land Processes Distributed Active Archive Center (LPDAAC).

References

Abdallah, C., Chorowicz, J., Bou, K.R., Khawlie, M., 2005. Detecting major terrain parameters relating to mass movements' occurrence using GIS, remote sensing and statistical correlations, case study Lebanon. *Remote Sens. Environ.*, **99**(4):448-461. [doi:10.1016/j.rse.2005.09.014]

Ahl, D.E., Gower, S.T., Mackay, D.S., Burrows, S.N., Norman, J.M., Diak, G.R., 2004. Heterogeneity of light use efficiency in a northern Wisconsin forest: implications for modeling net primary production with remote sensing. *Remote Sens. Environ.*, **93**(1-2):168-178. [doi:10.1016/j.rse.2004.07.003]

Bartelink, H.H., Kramer, K., Mohren, G.M.J., 1997. Applicability of the radiation-use efficiency concept for simulating growth of forest stands. *Agric. Forest Meteorol.*, **88**(1-4):169-179. [doi:10.1016/S0168-1923(97)00041-5]

Bonan, G.B., 1995. Land-atmosphere CO_2 exchange simulated by a land surface process model coupled to an atmospheric general circulation model. *J. Geophys. Res.*, **100**(D2):2817-2831. [doi:10.1029/94JD02961]

Canadell, J.G., Mooney, H.A., Baldochi, D.D., Berry, J.A., Ehleringer, J.R., Field, C.B., Gower, S.T., Hollinger, D.Y., Hunt, J.E., Jackson, R.B., *et al*., 2000. Carbon metabolism of the terrestrial biosphere: a multi-technique approach for improved understanding. *Ecosystems*, **3**(2):115-130. [doi:10.1007/s100210000014]

Ciais, P., White, J.W.C., Trolier, M., Francey, R.J., Berry, J.A., Randall, D.R., Sellers, P.J., Collatz, J.G., Schimel, D.S., Tans, P.P., 1995. Partitioning of ocean and land uptake of CO_2 as inferred by delta-C-13 measurements from the NOAA climate monitoring and diagnostics laboratory global air sampling network. *J. Geophys. Res.*, **100**(D3):5051-5070. [doi:10.1029/94JD02847]

Fang, J., Piao, S., Tang, Z., Peng, C., Ji, W., 2001. Interannual variability in net primary production and precipitation. *Science*, **293**(5536):1723a. [doi:10.1126/science.293.5536.1723a]

Field, C.B., Randerson, J.T., Malmström, C.M., 1995. Global net primary production: combining ecology and remote sensing. *Remote Sens. Environ.*, **51**(1):74-88. [doi:10.1016/0034-4257(94)00066-V]

Fik, T.J., Mulligan, G.F., 1998. Functional form and spatial interaction models. *Environ. Plan. A*, **30**(8):1497-1507. [doi:10.1068/a301497]

Foley, J.A., 1994. Net primary productivity in the terrestrial biosphere: the application of a global model. *J. Geophys. Res.*, **99**(D10):20773-20783. [doi:10.1029/94JD01832]

Hou, G.L., Li, J.Y., Zhang, Y.G., 1993. China Agro-meteorology Resources. China Remin University Press, Beijing, China (in Chinese).

Hu, Z.Z., Sun, J.X., Zhang, Y.S., 1990. Preliminary studies on calorific value and nutrient composition in Tianzhu alpine *Polygonum viviparum* meadow. *Acta Phytoecologica et Geobotanica Sinica*, **14**(2):185-190.

Huete, A.R., Didan, K., Miura, T., Rodriguez, X., Gao, X., Ferreira, L.G., 2002. Overview of the radiometric and biophysical performance of the MODIS vegetation indices. *Remote Sens. Environ.*, **83**(1-2):195-213. [doi:10.1016/S0034-4257(02)00096-2]

Hunt, E.R., 1994. Relationship between woody biomass and PAR conversion efficiency for estimating net primary production from NDVI. *Int. J. Remote Sens.*, **15**(8):1725-1730. [doi:10.1080/01431169408954203]

Jensen, M.E., Burman, R.D., Allen, R.G., 1990. Evapotranspiration and Irrigation Water Requirements. ASCE Manuals and Reports on Engineering Practice No. 70. American Society of Civil Engineers, New York, USA, p.112-131.

Keeling, C.D., Chin, J.F.S., Whorf, T.P., 1996. Increased activity of northern vegetation inferred from atmospheric CO_2 measurements. *Nature*, **382**(6587):146-148. [doi:10.1038/382146a0]

Kindermann, J., Wurth, G., Kohlmaier, G.H., Badeck, F.W., 1996. Interannual variation of carbon exchange fluxes in terrestrial ecosystems. *Global Biogeochem. Cy.*, **10**(4):737-755. [doi:10.1029/96GB02349]

Li, J., 2006. Study on the Spatial Distribution of Climatic Variables Based on GIS Technology and Its Application in Calculating Net Primary Productivity in China. PhD Thesis, Zhejiang University, Hangzhou, China (in Chinese).

Lieth, H., 1975. Modeling the Primary Productivity of the World. *In*: Lieth, H., Whittaker, R.H. (Eds.), Primary Productivity of the Biosphere. Springer, New York, USA, p.237-263.

Liu, S.R., Xu, D.Y., Wang, B., 1993. Impacts of climate change on productivity of forests in China 1: geographic distribution of actual productivity of forest in China. *Forest Res.*, **6**(6):634-642 (in Chinese).

Liu, X.A., Yu, G.C., Fan, L.S., Li, Z.Q., He, H.L., G, X.B., Ren, C.Y., 2004. Study on spatialization technology of terrestrial eco-information in China (III): temperature and precipitation. *J. Nat. Resourc.*, **19**(6):818-825 (in Chinese).

López-Blanco, J., Villers-Ruiz, L., 1995. Delineating boundaries of environmental units for land management using a geomorphological approach and GIS: a study in Baja California, Mexico. *Remote Sens. Environ.*, **53**(2):109-117. [doi:10.1016/0034-4257(95)00044-2]

Maisongrande, P., Ruimy, A., Dedieu, G., Saugier, B., 1995. Monitoring seasonal and interannual variations of gross primary productivity using a diagnostic model and remote-sensed data. *Tellus B*, **47**(1-2):178-190. [doi:10.1034/j.1600-0889.47.issue1.15.x]

Malmström, C.M., Thompson, M.V., Juday, G.P., Los, S.O., Randerson, J.T., Field, C.B., 1997. Interannual variation in global-scale net primary production: testing model estimates. *Global Biogeochem. Cy.*, **11**(3):367-392. [doi:10.1029/97GB01419]

Mohamed, M.A.A., Babiker, I.S., Chen, Z.M., Ikeda, K., Ohta, K., Kato, K., 2004. The role of climate variability in the inter-annual variation of terrestrial net primary production (NPP). *Sci. Total Environ.*, **332**(1-3):123-137. [doi:10.1016/j.scitotenv.2004.03.009]

Neill, C., Piccolo, M.C., Steudler, P.A., Melillo, J.M., Feigl, B.J., Cerri, C.C., 1995. Nitrogen dynamics in soils of forests and active pastures in the Western Brazilian Amazon Basin. *Soil Biol. Biochem.*, **27**(9):1167-1175. [doi:10.1016/0038-0717(95)00036-E]

Peng, C.H., Apps, M.J., 1999. Modelling the response of net primary productivity (NPP) of boreal forest ecosystems to changes in climate and fire disturbance regimes. *Ecol. Model.*, **122**(3):175-193. [doi:10.1016/S0304-3800(99)00137-4]

Peng, D.L., Huang, J.F., Wang, X.Z., 2007a. Correlative analysis between regional vegetation seasonal fluctuation and climate factors based on MODIS-EVI. *Chin. J. Appl. Ecol.*, **18**(5):983-989 (in Chinese).

Peng, D.L., Huang, J.F., Cai, C.X., Deng, R., 2007b. Spatialization on monthly average air temperature in Xinjiang and the analysis of the result. *J. Zhejiang Univ. (Sci. Ed.)*, **34**(5):580-584 (in Chinese).

Peng, D.L., Huang, J.F., Cai, C.X., Deng, R., Xu, J.F., 2008. Assessing the response of seasonal variation of net primary productivity to climate using remote sensing data and geographic information system techniques in Xinjiang. *J. Integr. Plant Biol.*, **50**(12):1580-1588. [doi:10.1111/j.1744-7909.2008.006 96.x]

Ruimy, A., Kergoat, L., Bondeau, A., 1999. Comparing global models of terrestrial net primary productivity (NPP): analysis of differences in light absorption and light-use efficiency. *Global Change Biol.*, **5**(Suppl. 1):56-64. [doi:10.1046/j.1365-2486.1999.00007.x]

Running, S.W., Nemani, R.R., Heinsch, F.A., Zhao, M.S., Reeves, M., Hashimoto, H., 2004. A continuous satellite-derived measure of global terrestrial primary productivity: future science and applications. *Bioscience*, **54**(6):547-560. [doi:10.1641/0006-3568(2004)054[0547:ACSMOG]2.0.CO;2]

Steele, B.M., Reddy, S.K., Nemani, R.R., 2005. A regression strategy for analyzing environmental data generated by spatio-temporal processes. *Ecol. Model.*, **181**(2-3):93-108. [doi:10.1016/j.ecolmodel.2004.06.038]

Sun, H.S., Huang, J.F., Huete, R.A., Peng, D.L., Zhang, F., 2009. Mapping paddy rice with multi-date moderate-resolution imaging spectroradiometer (MODIS) data in China. *J. Zhejiang Univ.-Sci. A*, **10**(10):1509-1522. [doi:10.1631/jzus.A0820536]

Sun, R., 1998. Research of the Terrestrial Vegetation Net Primary Production (NPP) in China Base on AVHRR-NDVI. PhD Thesis, Beijing Normal University, Beijing, China (in Chinese).

Sun, R., Zhu, Q.J., 2000. Distribution and seasonal change of net productivity in China from April, 1992 to March, 1993. *J. Geograph. Sci.*, **55**(1):36-45 (in Chinese).

Sun, R., Zhu, Q.J., 2001. Effect of climate change of terrestrial net primary productivity in China. *J. Remote Sens.*, **5**(1):58-62 (in Chinese).

Tian, H., Melillo, J.M., Kicklighter, D.W., McGuire, A.D., Helfrich, J.V.K., Moore, B., Vörösmarty, C.J., 1998. Effect of interannual climate variability on carbon storage in Amazonian ecosystems. *Nature*, **396**(6712):664-667. [doi:10.1038/25328]

Turner, D.P., Gower, S.T., Cohen, W.B., Gregory, M., Maiersperger, T.K., 2002. Effects of spatial variability in light use efficiency on satellite-based NPP monitoring. *Remote Sens. Environ.*, **80**(3):397-405. [doi:10.1016/S0034-4257(01)00319-4]

Wang, F.M., Huang, J.F., Zhou, Q.F., Wang, X.Z., 2008. Optimal waveband identification for estimation of leaf area index of paddy rice. *J. Zhejiang Univ.-Sci. B*, **9**(12):953-963. [doi:10.1631/jzus.B0820211]

Wolfgang, C., 1999. Net primary productivity model intercomparison activity. *Gobal. Change Biol.*, **5**(Suppl. 1):4-6.

Yu, G.C., He, H.L., Liu, X.A., 2004. Atlas for Spatialized Information of Terrestrial Ecosystem in China: Volume of Climatological Elements. Weather Press, Beijing, China, p.18-169 (in Chinese).

Zhang, H., Gao, S.Y., Zheng, Q.H., 2002. Responses of NPP of salinized meadows to global change in hyperarid regions. *J. Arid Environ.*, **50**(3):489-498. [doi:10.1006/jare.2001.0863]

Zhang, X.X., Ge, Q.S., Zheng, J.Y., 2005. Impacts and lags of global warming on vegetation in Beijing for last 50 years based on remotely sensed data and phonological information. *Acta Ecologica Sin.*, **24**(2):123-130 (in Chinese).

Zhao, M.S., Running, S.W., 2006. Sensitivity of moderate resolution imaging (MODIS) terrestrial primary production to the accuracy of meteorological re-analyses. *J. Geophys. Res.*, **111**(G1):G01002. [doi:10.1029/2004JG000004]

Zhao, M.S., Heinsch, F.A., Nemani, R.R., Running, S.W., 2005. Improvements of the MODIS terrestrial gross and net primary production global data set. *Remote Sens. Environ.*, **95**(2):164-176. [doi:10.1016/j.rse.2004.12.011]